

Manuscript Number: CARBPOL-D-19-00362R2

Title: Drug micro-carriers with a hyaluronic acid corona toward a diffusion-limited aggregation within the vitreous body

Article Type: Research Paper

Keywords: hyaluronic acid; microparticle; PLGA; poloxamer; diffusion; ocular delivery.

Corresponding Author: Dr. Laura Mayol,

Corresponding Author's Institution: University of Naples Federico II

First Author: Laura Mayol

Order of Authors: Laura Mayol; Teresa Silvestri; Sabato Fusco; Assunta Borzacchiello; Giuseppe De Rosa; Marco Biondi

Abstract: Posterior eye segment diseases are treated through monthly intravitreal injections, that evoke serious side effects. A promising approach to reduce injection frequency consists in producing biodegradable microspheres (MPs) releasing the protein in the vitreous body for long times. Moreover, a rational design of these MPs requires a discouraged diffusion/sedimentation within the intravitreal space, which are detrimental for the vision and the control over drug release kinetics. In this work, poly(lactic-co-glycolic acid) (PLGA)-based MPs encapsulating bovine serum albumin (BSA) were coated with hyaluronic acid (HA) at two molecular weights and tested for their release, diffusion and degradation features in simulated vitreous body (SVB). Results indicate that HA corona prolongs MP degradation time and BSA release. Furthermore, HA coating increased the affinity between MPs and SVB, thereby repressing device transport compared to control PLGA MPs. Results hold promise for the possible application of HA-decorated MPs for intravitreal injection of protein drugs.

*Highlights (for review)

- Microparticles were decorated with two different molecular weights hyaluronic acid
- Hyaluronic acid corona discourage the diffusion of microparticles in the vitreous
- The molecular weight of the hyaluronic acid influence protein release kinetics
- Hyaluronic acid molecular weight influence the diffusion of the microparticles
- Hyaluronic acid molecular weight does not affect degradation time of microparticles

Dear Editor, we are grateful for the accurate and thoughtful comments to our manuscript, which allowed us to significantly improve its quality. In the following, there is a point-by-point answer to referee considerations.

Reviewer #1: The authors revised the manuscript as per the reviewer's suggestions/recommendations. Now the manuscript can be accepted for publication in this journal.

Reviewer #2: The authors have responded to my questions in a good manner.

I have only 2 additional questions:

1. the loading capacity of the BSA in PLGA is stated at 76% in table 1, while the text states 36% efficiency. Which one is correct?

We are sorry for the oversight that has been corrected.

2. Figure 4. Temporal release trends of BSA from MPs over time: the PLGA particles show a plateau from day 20, is this corresponding to 100% release? Could you convert the Y-axis also to percentage (or discuss how the doses in the Y-axis correspond to the BSA percentage loaded in the particles) to estimate which amount of the loaded dose has been released?

As suggested by the referee, we converted the Y-axis to percentage released.

1 **Drug micro-carriers with a hyaluronic acid corona**
2 **toward a diffusion-limited aggregation within the**
3 **vitreous body**

4 Laura Mayol^{1,2,*}, Teresa Silvestri¹, Sabato Fusco², Assunta Borzacchiello³,
5 Giuseppe De Rosa^{1,2}, Marco Biondi^{1,2}

6
7
8 ¹ Dipartimento di Farmacia, Università di Napoli Federico II, Via D. Montesano 49, Napoli, Italy.

9 ² Interdisciplinary Research Centre on Biomaterials – CRIB – Università di Napoli Federico II –
10 P.le Tecchio, 80, Napoli, Italy

11 ³ Istituto per i Materiali Compositi e Biomedici (IMCB-CNR), Università di Napoli Federico II,
12 Viale J.F. Kennedy , Napoli, Italy

13 *Correspondence to:

14 Laura Mayol, Dipartimento di Farmacia, Scuola di Medicina e Chirurgia, Università di Napoli
15 Federico II, Via D. Montesano 49, Napoli, Italy. Mail: laumayol@unina.it

16

17 **Abstract**

18 Posterior eye segment diseases are treated through monthly intravitreal injections, that evoke
19 serious side effects. A promising approach to reduce injection frequency consists in producing
20 biodegradable microspheres (MPs) releasing the protein in the vitreous body for long times.
21 Moreover, a rational design of these MPs requires a discouraged diffusion/sedimentation within the
22 intravitreal space, which are detrimental for the vision and the control over drug release kinetics. In
23 this work, poly(lactic-co-glycolic acid) (PLGA)-based MPs encapsulating bovine serum albumin
24 (BSA) were coated with hyaluronic acid (HA) at two molecular weights and tested for their release,
25 diffusion and degradation features in simulated vitreous body (SVB). Results indicate that HA
26 corona prolongs MP degradation time and BSA release. Furthermore, HA coating increased the
27 affinity between MPs and SVB, thereby repressing device transport compared to control PLGA
28 MPs. Results hold promise for the possible application of HA-decorated MPs for intravitreal
29 injection of protein drugs.

30

31

32

33

34

35

36 **Keywords:** hyaluronic acid, microparticle, PLGA, poloxamer, diffusion, ocular delivery.

37

38 **1. Introduction**

39 Posterior eye segment diseases can be treated in principle through four routes of administration, i.e.
40 topical, systemic, intraocular and periocular (Herrero-Vanrell et al., 2001). The systemic route
41 requires high drug doses to achieve therapeutic drug levels in the eye and this correlates with a high
42 risk of eliciting systemic adverse effects; the topical and periocular routes are progressively gaining
43 more attention, but the intravitreal injection is still the most employed since the active molecules are
44 directly inserted into the vitreous, thereby overcoming the numerous biological barriers hampering
45 the access of drugs and molecules within the eye (Gaudana et al., 2010; Falavarjani et al., 2013).
46 Unfortunately, even if intravitreal injection is actually a very effective route of administration, it
47 educes serious drawbacks. First, drug distribution in the vitreous is non-uniform: for example, small
48 molecules can rapidly diffuse through the vitreous, whereas the transport of larger molecules is
49 restricted. Besides, intravitreal injection is intrinsically associated to pernicious adverse effects,
50 such as cataracts, retinal detachment, and hemorrhages, and the risk of their occurrence is
51 increasing with increasing number of injections (Herrero-Vanrell et al., 2000). Consequently, the
52 use of biodegradable controlled drug delivery systems (DDS) based on FDA-approved
53 biodegradable polyesters such as poly(lactic-co-glycolic acid) (PLGA) for intravitreal injection is
54 very attractive. Specifically, micron-sized particulate DDS, such as microparticles (MPs), are
55 beneficial since they allow the co-administration of more than one active molecule, and help
56 avoiding the surgical procedures needed to reach the intraocular target site. More importantly,
57 biodegradable MPs can host, protect and sustain the release kinetics of the encapsulated drug(s),
58 thereby leading to a reduction of the frequency of intravitreal injections and of the concentration
59 peaks of the active molecule(s) in the intravitreal space, hence involving a minor risk of adverse
60 effect insurgence (Yasukawa T et al., 2011). A personalized therapy can be easily realized by
61 tailoring the amount of administered MPs and, hereafter, drug dosing. Also, biodegradable PLGA-
62 based MPs are well tolerated after periocular and intravitreal injections in both animals and humans.

63 Indeed, the systemic toxicity of PLGA is basically negligible since the polymer is easily hydrolyzed
64 *in vivo* to lactic and glycolic acid, which are then eliminated as carbon dioxide and water via the
65 Krebs cycle (Danhier et al., 2012). For these reasons, presumably a variety of microparticulate
66 formulations for different ophthalmic therapeutic uses will soon be available in the clinical practice
67 (Herrero-Vanrell et al., 2014). After injection, PLGA-based MPs can behave like an ‘*in situ*-
68 forming’ implant, since they easily undergo aggregation. This has two conflicting implications: on
69 the one side, MP aggregation at the site of the injection allows a free visual axis within the vitreous
70 body; on the other hand, MP aggregation results into a less effective control over drug release
71 kinetics, and this is strongly unwished for intravitreal administration. Consequently, it is desirable
72 that MPs are separated during all the drug release phase and motionless within the intravitreal
73 space. The vitreous body has a gel structure, it is composed almost completely of water (97%) and
74 three main components: collagens, proteoglycans and HA. Among its macromolecular components,
75 HA is present in high amount and it is thought to control many vitreous biophysical properties such
76 as its viscoelastic properties that enable it to resist sudden compression shocks, offering the best
77 protection for the retina.

78 Here, we present the preparation of biodegradable PLGA-based MPs, whose surface properties have
79 been tailored to make the devices motionless within the intravitreal space. More in detail, we have
80 decorated the external surface of these polymeric MPs with hyaluronic acid (HA). HA is a natural
81 mucoadhesive polysaccharide, widely used in drug delivery and biomedical field, composed of
82 alternating D-glucuronic acid (GlcA) and N-acetyl-D-glucosamine (GlcNAc) repeating units linked
83 together via β -(1,4) and β -(1,3) glycosidic junctions. In aqueous solution, HA can bind and interact
84 with water molecules and also entangle with other HA macromolecules, by that being responsible
85 for the viscoelastic behavior of many biological fluids besides vitreous body, such as synovial fluid,
86 tears etc (Mayol et al., 2014; Borzacchiello et al., 2010). Thus, here we have speculated that, by
87 increasing the chemical affinity of the MP surface with the surrounding body fluid, the diffusion of

88 the MP in the vitreous body would be discouraged as a consequence of HA macromolecules ability
89 to interact and entangle with one another.

90 The MPs here produced were loaded with bovine serum albumins (BSA) and fully characterized for
91 their technological features. Then, the degradation properties of the MPs were analyzed since this is
92 a crucial feature for their ability to prolong the release of the drug into the eye which, in turn, is
93 expected to decrease the frequency of injection and reduce the adverse effects due to drug
94 intravitreal injections. Finally, the influence of HA molecular weight on MP surface on both drug
95 release kinetics and MP diffusion in simulated vitreous body was explored.

96

97 **2. Materials and Methods**

98 *2.1. Materials*

99 HA with a weight-average molecular weight (MW) of 1600 kDa and 180 kDa was provided by
100 Altergon Italia s.r.l (Italy). Equimolar uncapped poly(D,L-lactic-co-glycolic acid) (PLGA)
101 (Resomer RG504H, Mw 40 kDa, inherent viscosity: 0.16-0.24 dL g⁻¹ in acetone at 25 °C) was from
102 Evonik (Germany). Poloxamers (PEO_a-PPO_b-PEO_a), which are amphiphilic triblock polymers
103 containing different numbers of oxyethylene (a) and oxypropylene (b) units, were used. In this
104 work, poloxamers F127 (a = 100 and b = 65) and F68 (a = 76 and b = 29) from Lutrol (BASF,
105 Germany) were employed. All other chemicals, i.e. bovine bovine serum albumins (BSA), ethanol
106 (EtOH), acetone, dimethylsulfoxide (DMSO), dichloromethane (DCM), poly (vinyl alcohol) (PVA:
107 Mowiol 40-88) sodium azide, Agar, rhodamine, phosphate buffer salts, sodium and potassium
108 chloridrate (PBS) were obtained from Sigma–Aldrich (USA).

109 *2.2. Microparticle production*

110 MPs loaded with BSA were produced with a theoretical protein loading of 0.2% (0.20 mg of BSA
111 *per* 100 mg of microparticles), using a slightly modified double emulsion–solvent evaporation
112 technique. Briefly, 0.25 mL of an internal aqueous phase consisting of a BSA solution (0.4% w/v)
113 in phosphate buffer (PBS, 1.420 g of Na₂HPO₄, 0.201 g of KCl and 7 g of NaCl in 1 L of purified
114 H₂O) were poured into 2.5 mL of a 20% w/v organic solution of PLGA/F68/F127 (1:0.5:0.5 weight
115 ratio) in dichloromethane (DCM). When necessary, 5 µL of a rhodamine solution in DCM (0.1%
116 w/v) were added to the organic phase to obtain fluorescent particles used in diffusion studies. The
117 two phases were then emulsified by a high-speed homogenizer (Dixax 900 equipped with a 10G
118 probe, Heidolph, Germany; 11,000 rpm, 2 min) and the obtained water-in-oil primary emulsion was
119 poured in 40 mL of an external aqueous phase and further homogenized at 11,000 rpm (10G probe)
120 for 2 minutes, to obtain the final double emulsion. The external aqueous phase contained 7.5 mg of
121 F68, 7.5 mg of F127 and 30 mg of hyaluronic acid. In the case of control PLGA MPs, the organic
122 phase was a 20% w/v solution of PLGA in DCM, while the external aqueous phase was produced
123 without HA. The organic solvent was then evaporated overnight under magnetic stirring (MR 3001
124 K, Heidolph, Germany) at room temperature for MP hardening, which were finally centrifuged
125 (5000 rpm, 4°C), washed with distilled water three times (Universal 16R, Hettich Zentrifugen,
126 Germany) and lyophilized for 24 h (0.01 atm, -60 ° C) (Modulyo, Edwards, United Kingdom). As a
127 control, PLGA MPs were produced without HA. In that case, the organic phase was composed of a
128 20% w/v solution of PLGA in DCM, and the external aqueous phase contained F68 and F127
129 poloxamers.

130 *2.3. Microparticle morphology and size*

131 Scanning electron microscopy (SEM) (Phenom XL, Phenom World, the Netherlands) was
132 employed to analyze microsphere external shape and morphology after production. The samples
133 were prepared by gold-sputtering under vacuum. The mean volume and size distribution of the
134 produced MPs were determined by light scattering (Microtrac S3500 Series Particle Size Analyzer;

135 Montgomeryville, PA, USA). The tests were run by dispersing lyophilized MPs in MilliQ water
136 containing 0.5% w/v PVA, which was used as a surface active agent to prevent MP aggregation
137 during the measurements. The results and the standard deviation have been averaged on triplicate
138 samples.

139 *2.4. MP yield and entrapment efficiency*

140 MP yield was gravimetrically obtained from the entire mass of MPs recovered after lyophilization
141 ($p < 5$ hPa, 24 h; LyoQuest, Telstar, Japan). Direct method was employed to obtain the amount of
142 BSA loaded into the MPs, by means of Bradford assay (Noble, Bailey; 2009). More in detail, for
143 each experiment 10 mg of MPs were added to 500 μ L of dichloromethane. Then, 100 μ L of PBS
144 (pH = 7.4) were added to the obtained organic solution and vortexed for 5 s to enhance an intimate
145 contact between the aqueous and the organic phases. Afterwards, 50 μ L of the aqueous solution
146 were withdrawn and diluted within 950 μ L of the Bradford reagent for 15 min. BSA was quantified
147 *via* spectrophotometric assay (UV-1800, Shimadzu; $\lambda = 595$ nm, Figure 3.3), employing a quartz
148 cuvette (6030-UV, $d = 10$ mm, Hellma Analytics). The linearity of the response was assessed in the
149 0.49-500 μ g/mL BSA concentration range ($r^2 > 0.98$). Results are expressed as actual BSA loading
150 (mg of loaded BSA *per* 100 mg of MPs), and BSA encapsulation efficiency (ratio of actual and
151 theoretical BSA loading rate $\times 100$) \pm standard deviation of the values collected from at least three
152 different batches.

153 *2.5. Preparation of simulated vitreous body (SVB)*

154 Simulated vitreous body (SVB), prepared following a previously published procedure (Kummer et
155 al., 2007). Briefly, a solution composed of 0.4 g of Agar and 100 mL of water was lead to boiling
156 up until complete Agar dissolution. Subsequently, the hot solution was mixed with 0.5 g of HA
157 (1600 kDa) until a homogeneous mixture was obtained. A few drops of 0.02% w/v sodium azide

158 solution were added to the obtained solution as a preservative and, then, the solution was cooled to
159 room temperature for 24h.

160 *2.6. Rheological properties of SVB*

161 The viscoelastic properties of the prepared SVB were measured by a Kinexus rotational rheometer
162 (Malvern, USA). More in detail, small-amplitude oscillatory shear experiments were performed at
163 37°C in the 0.1 to 10 Hz oscillation frequency range, and at a strain amplitude at which linear
164 viscoelasticity was attained. The dynamic viscosity was, then, measured as a function of frequency.

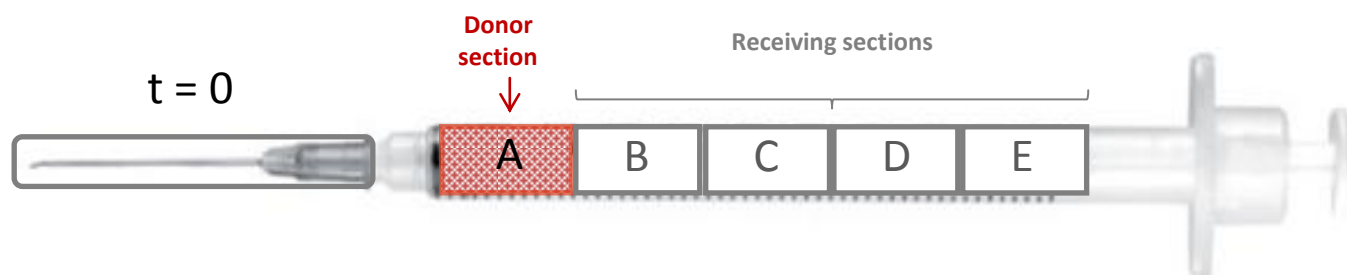
165 *2.7 – BSA release kinetics*

166 The *in vitro* release profile of BSA from control PLGA MPs and HA-decorated MPs in SVB was
167 evaluated by the gel poured into a vial and adding the HA-decorated MPs at a 1:20 w/v ratio. The
168 MPs and the gel were accurately mixed until a uniform suspension was obtained. Subsequently, 1
169 mL of PBS at pH 7.4 was added on the gel containing the dispersed MPs. and placed at 37°C in a
170 thermostatic bath. At predetermined time points, 500 µL aliquots of the supernatant were withdrawn
171 and replaced with fresh PBS, and pH values were verified using litmus paper. 50 µL of solution
172 were withdrawn and placed in contact with 950 µL of Bradford and quantified by
173 spectrophotometric assay, as described in Section 2.4. The linearity of response was assessed in the
174 0.5-500 µg/mL BSA concentration range ($r^2 > 0.99$). The results were expressed in terms of the
175 percentage of released BSA \pm the standard deviation of three replicates.

176 *2.8. Transport studies of MPs in SVB*

177 Transport properties of MPs in SVB have been studied through fluorescence measurements.
178 Fluorescent MPs loaded with rhodamine (Rhod) were produced as described in Section 2.2.
179 Subsequently, they have been evenly incorporated in the produced SVB (2% w/v) and 200 µL
180 aliquots of this dispersion were placed in the donor chamber of a 1 mL plastic syringe, preliminarily
181 cut in five equal sections (Figure 1). Consequently, the system was composed of one donor section

182 and four receiving sections. Adjacent sections were separated by a nylon web (approximately 0.5
183 mm average mesh aperture) to enhance an even separation between the sections.



184

185 *Figure 1. Schematic representation of the diffusion study apparatus.*

186

187 All the syringes were kept in vertical position, with the tip accurately sealed to avoid SVB loss
188 during the experiments. The top section of each syringe, acting as the donor compartment,
189 contained a 4 mg/ml dispersion of Rhod-loaded MPs in SVB. Then, the syringes were placed at
190 37°C and, at scheduled time intervals, the syringes were withdrawn, and the single sections
191 separated and immediately frozen at -20°C to anneal further transport. Then, the syringe was
192 divided into single sections. The content of each section was dissolved in 2 mL NaOH 0.5 N and
193 analyzed for Rhod content by spectrofluorimetric analysis at $\lambda = 553$ nm (Varian Cary Eclipse
194 Fluorescence Spectrophotometer, Thermofisher, USA), using a quartz cuvette (6030-UV, d = 10
195 mm, Hellma Analytics, USA). The linearity of the response was assessed in the 0.125 – 2 mg/mL
196 MP concentration range ($r^2 > 0.99$).

197 2.8. Mass loss kinetics of MPs

198 The rate of mass loss of the MP decorated with HA molecular weight equal to 180 or 1600 kDa
199 were performed. In detail, 0,5% w/v suspensions of MPs in PBS were prepared and subsequently
200 incubated at 37°C on a gently oscillating base (15 rpm) (Stovall Life Science Inc., USA). At
201 scheduled time points, the samples were centrifuged (5000 rpm, 10 minutes) and the PBS

202 supernatant, containing the solubilized MP fractions, was withdrawn and replaced with an equal
203 volume of fresh PBS. Then, the samples were lyophilized (LyoQuest, Telstar, Japan) and the
204 residual weight was gravimetrically obtained, taking into account the mass of the salts,
205 preliminarily determined by lyophilizing PBS solutions used as a control (n = 6). The results have
206 been expressed as the mean residual mass percentage \pm the standard deviations of at least three
207 replicas.

208 $100 \times \left(1 - \frac{MP\ Mass\ t_0}{Residual\ MP\ Mass}\right) .$

209

210 **3. Results and discussions**

211 The aim of this work was the development of a biodegradable MP platform designed to be
212 motionless within the ocular vitreous body and able to sustain and control the drug release phase,
213 thus reducing the frequency of intravitreal injections and, consequently, the occurrence of the
214 associated risks (Adamson et al., 2016). The MPs decorated with HA were produced by a slightly
215 modified double emulsion – solvent evaporation technique. HA was added to the external aqueous
216 phase to promote its interaction with the organic phase containing the blend of lipophilic PLGA and
217 amphiphilic poloxamers. During the second emulsification step, the droplets of the internal organic
218 solution spontaneously orient the hydrophilic segments of the poloxamers towards the external
219 aqueous phase containing HA, and this is expected to be decisive in promoting the HA arrangement
220 on the surface of the MPs, driven by the lipophilicity gradient between the organic and the aqueous
221 phase of the emulsion (Giarra et al., 2016), after the evaporation of the organic solvent. More in
222 detail, HA was chosen because it is a major component of the vitreous body, and this is expected to
223 increase MP affinity with the surrounding gel containing the same polysaccharide. In this work, it
224 has been hypothesized that this affinity of composition between the surface of the MP and the
225 vitreous body may hinder the diffusion/sedimentation and aggregation of MP within the ocular
226 vitreous. A further objective of this work was to evaluate if the molecular weight of the HA used to
227 decorate the surface can influence the degradation and diffusion of the MP in the simulated vitreous
228 body (SVB), as well as on the release kinetics of the loaded protein. It must be underlined that, for a
229 possible clinical application, the site of injection of MPs must be properly chosen to avoid the risk
230 of vision blurring. In this perspective, a successful treatment based on intravitreal MP injection is
231 strictly related on MP injection outside the visual path within the eye. For this reason, negligible
232 diffusion features of MPs in the long time are necessary to ensure a significance of the treatment
233 (Wang et al., 2014; Zhang et al., 2015). The SVB was prepared according to the procedures
234 reported in the literature and, before the release and diffusion studies, we verified that its

235 rheological properties were close to those of the human vitreous body (data not shown) (Soman et
236 al., 2003).

237 3.1. MP characterisation

238 In table 1, the acronyms, mean diameter and BSA entrapment efficiency of the prepared
239 formulations are summarized.

240

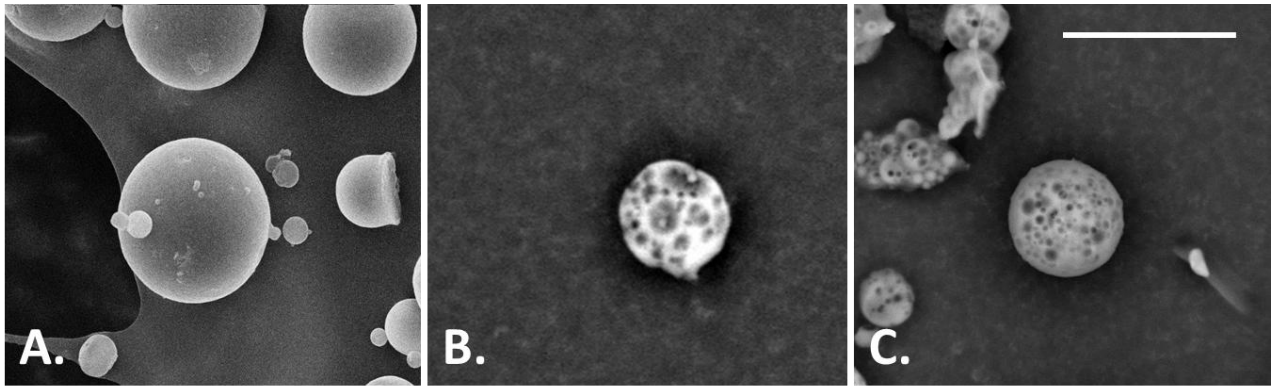
Formulation	Hyaluronic acid molecular weight [kDa]	Mean diameter [μm] (\pm S.D.)*	BSA entrapment efficiency [%] (\pm S.D.)
PLGA	-	8.3 (\pm 1.7)	76 (\pm 4)
HA180	180	9.0 (\pm 1.2)	85 (\pm 11)
HA1600	1600	8.7 (\pm 1.1)	88 (\pm 12)

241 * Standard deviation is calculated on 10 different batches

242 *Table 1.: Overall technological features of the produced MPs.*

243

244 As shown in Table 1, the adopted formulation conditions allowed to obtain MPs with a mean
245 diameter around 9 μm , able to encapsulate BSA with > 76% efficiency in all cases. As clearly
246 revealed by SEM images, the produced PLGA MPs were spherical with a smooth surface (figure
247 2A) while HA containing formulations presented a porous surface (figures 2 B and C).

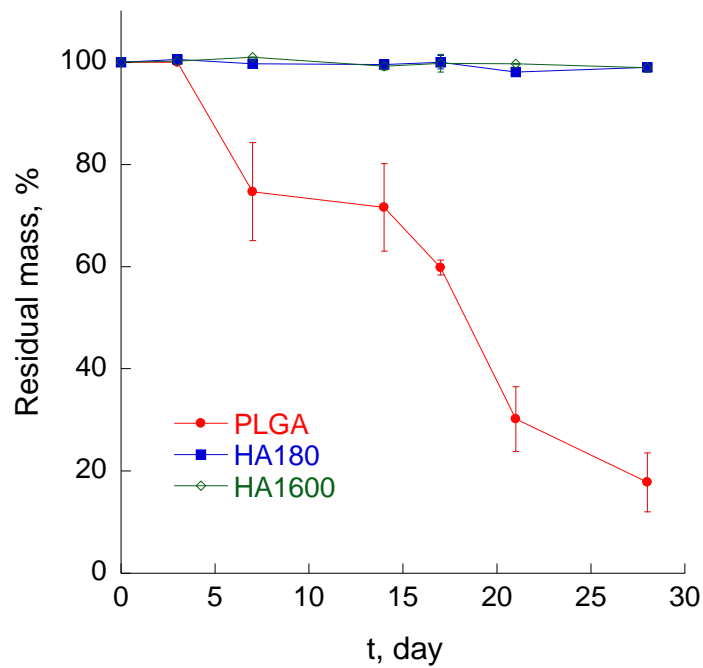


248

249 *Figures 2: Representative SEM images of (A) PLGA (B) HA180 and (C) HA 1600 MPs. The bar is*
 250 *10 μ m.*

251 *3.2. Degradation studies of MPs*

252 As described in the Section 2.8, the mass loss/degradation kinetics have been observed through a
 253 0.5% w/v MPs suspension in PBS incubated at 37°C. At scheduled time points, the residual mass of
 254 the MPs was gravimetrically obtained on the lyophilized residue, taking into account the salts mass.



255

256

Figure 3: MP time trend of mass loss.

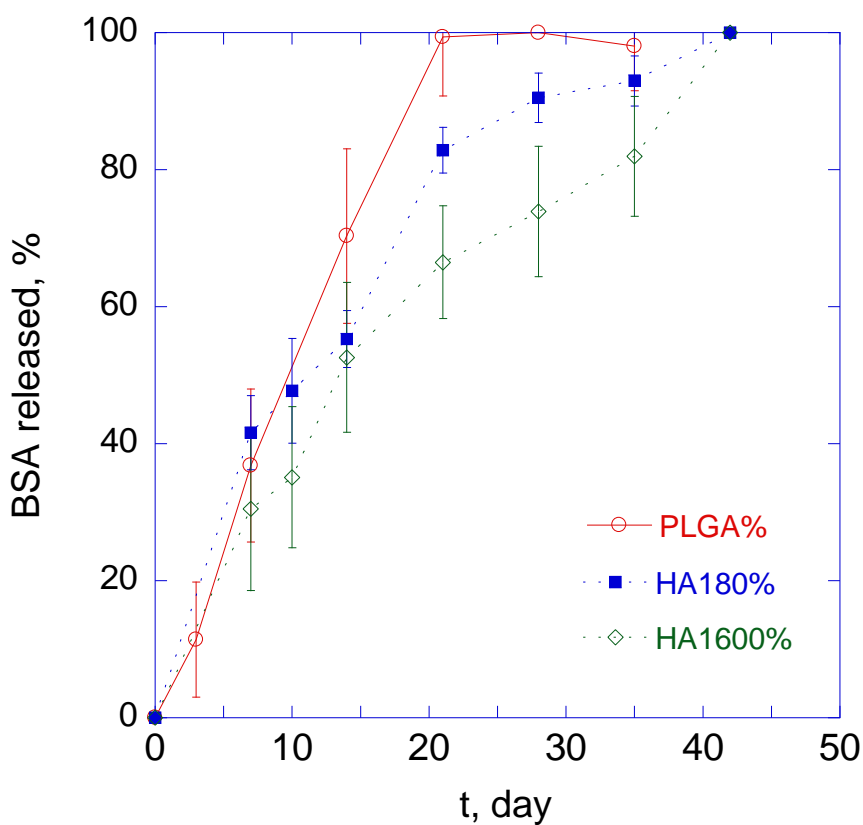
258 Per cent changes in MP mass were calculated as the rate of material loss during the incubation of
259 the devices over a 4-week course *in vitro*. The trend of MP mass loss is presented in Fig. 3.

260 Autocatalytic PLGA degradation can be schematized as follows: (i) initially, water invades the
261 polymeric matrix due to MP porous structure which allows a fast water penetration (Tamada et al.,
262 1992) and polymer plasticization (Blasi et al., 2005); (ii) then, hydrolysis-triggered PLGA
263 degradation at chain backbone takes place and, progressively, soluble acidic by-products are
264 formed; (iii) the produced acids catalyze degradation, thereby furthering the formation of additional
265 soluble acidic degradation products (Joshi, Himmelstein, 1991). It must be specified that, during
266 degradation, molecular weight steadily decreases, while device mass loss takes place when polymer
267 molecules reach a critical molecular weight below which PLGA oligomers are soluble.

268 The collected data display that in 28 days control PLGA MPs lost > 80% of their initial mass while,
269 in the same time frame, the overall mass of both HA-containing formulations was roughly constant,
270 with a loss of material around few per cent points. This indicates that, only in HA-containing
271 devices, the molecular weight of PLGA is still above the dissolution threshold value and, hence,
272 that the degradation rate for both formulations is definitely lower. Actually, poloxamers presence in
273 the bulk of MPs can be associated to a dilution of acidic degradation products, along with a
274 buffering effect which slow down the autocatalytic degradation of MPs. Furthermore, it must be
275 pointed out that MPs containing poloxamers are more hydrophilic compared to the devices made up
276 of bare PLGA and this is associated to a sensible enhancement of acidic degradation by-products
277 diffusion outwards to the surrounding gel. Furthermore, the results depicted in Fig. 3 show that the
278 presence of different molecular weight HA molecules on the surface has seemingly no effect on the
279 percentage of degradation in this first stage of HA containing MP degradation.

280 *3.3. Release studies of MPs in SVB*

281 In order to study the release features of the produced MPs decorated with HA in the ocular vitreous
282 body, control PLGA and HA-decorated MPs have been dispersed in SVB and the resulting MP-
283 loaded gel placed on the bottom of a vial, covered with PBS and incubated at 37 °C. The presence
284 of SVB ensures the interactions between the HA chains exposed upon MP surface and the HA
285 molecules contained in SVB. At scheduled time points, spectrophotometric analysis has allowed to
286 assess whether the molecular weight of HA coronas influenced drug release kinetics of BSA from
287 MPs. In figure 4, the release profiles of BSA from PLGA-based MPs, with or without external HA
288 (at 180 or 1600 kDa) corona, are reported.



289

290 *Figure 4. Temporal release trends of BSA from MPs over time.*

291

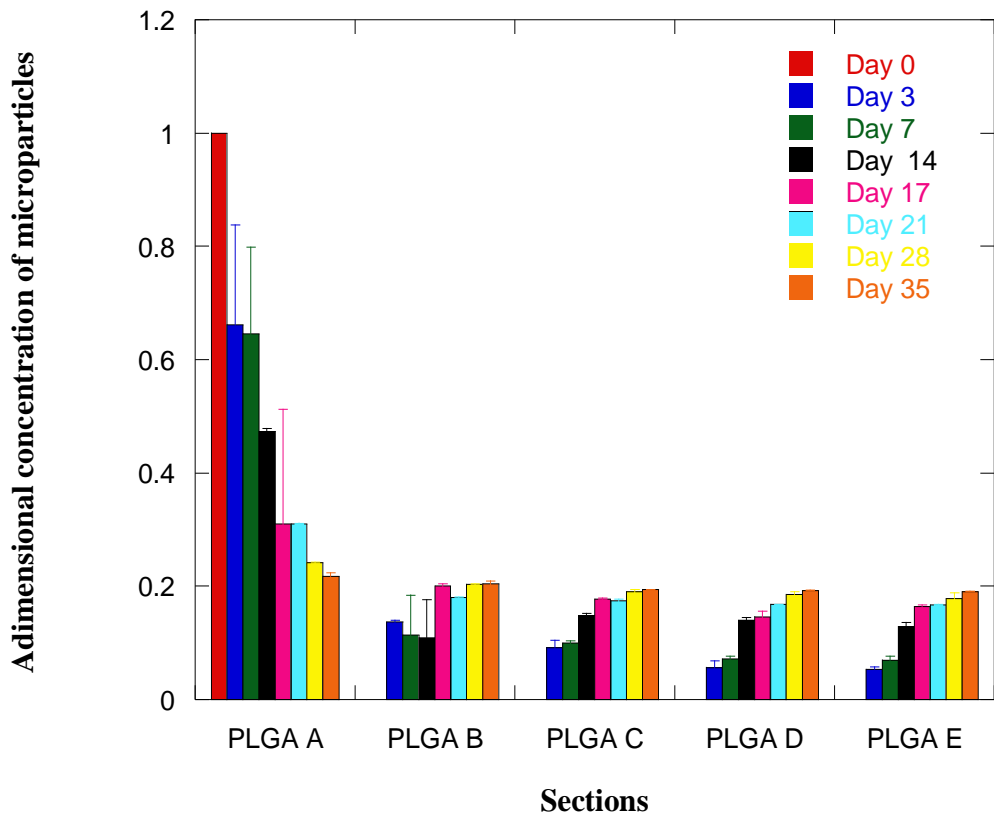
292 It is known that drug release from PLGA-based drug delivery systems is governed by a complex
293 mechanism deriving from the combination of drug diffusion through the polymeric matrix and the
294 concomitant polymer bulk degradation (Blasi *et al.*, 2005). Results indicate that PLGA MPs can
15

295 prolong BSA release phase for three weeks with a release curve, in this time frame, quite
296 superimposable to that obtained from HA1600 formulation and slower compared to HA180
297 formulation. Differently, both formulations with HA present qualitatively similar trends of protein
298 release kinetics, with a prolonged release phase for at least six weeks. Specifically, the amount of
299 protein released by HA1600 MPs was found to be lower compared to that released by HA180.
300 Therefore, a prolonged degradation time of MPs, due to the presence of poloxamers in the
301 formulation, contribute to sustain the release of the loaded drug molecule(s), thereby reducing the
302 frequency of intravitreal injections and the related risk of adverse effects. The different profile of
303 HA 180 and HA 1600 MPs can be related to the HA arrangement on MP surface. Indeed, high
304 molecular weight HA is constituted by longer chains which can form physical entanglements. This
305 feature may hinder the diffusion of the drug, thus slowing down drug release kinetics.

306 *3.4. Diffusion studies of fluorescent MPs*

307 MP size exceeds the vitreous mesh size (about 500 nm) and this clearly discourages their free
308 diffusion into the posterior segment of the eye (Xu et al., 2013). Thus, only MP sedimentation can
309 occur in a long time frame (up to some months of a sustained drug release), as a consequence of
310 viscous flow of macromolecules constituting the hydrogel matrix of the vitreous body. Hereafter,
311 the syringe technique was used to evaluate transport properties of MPs into SVB, thus mimicking
312 their sedimentation after the intravitreal injection of MPs. More in detail, diffusion tests of
313 fluorescent HA1600 and HA180 MPs in SVB were performed and compared to the transport
314 properties of MPs without HA corona (namely PLGA MPs) of comparable size. Results of diffusion
315 tests are presented in figures 5, 6 and 7.

316

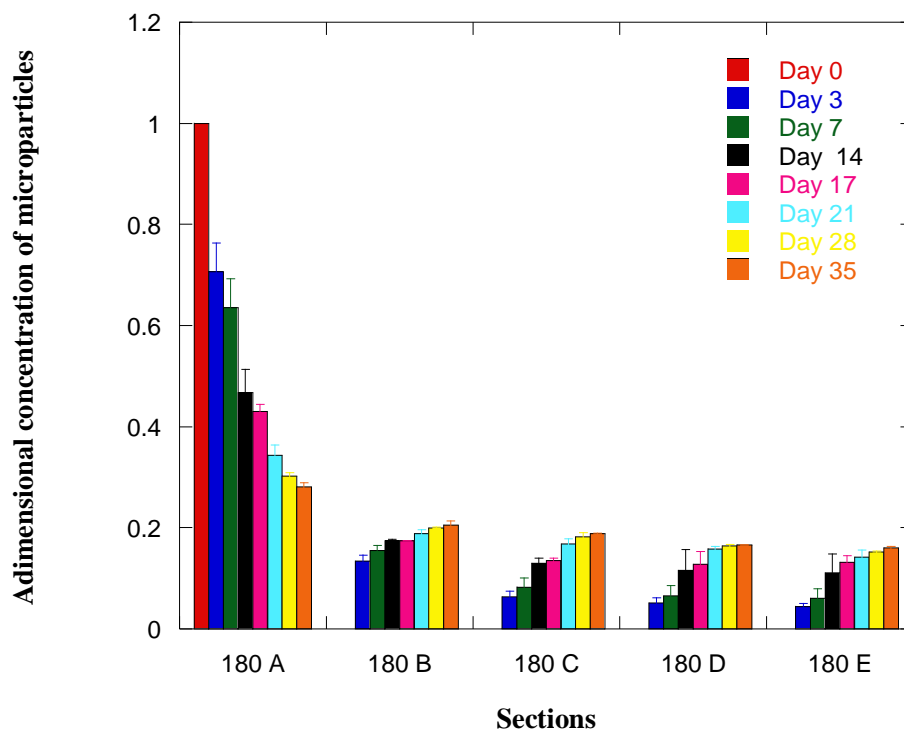


317
318

319

Figure 5: Diffusion test of PLGA MPs.

320



321
322

Figure 6: Diffusion test of HA180 MPs.

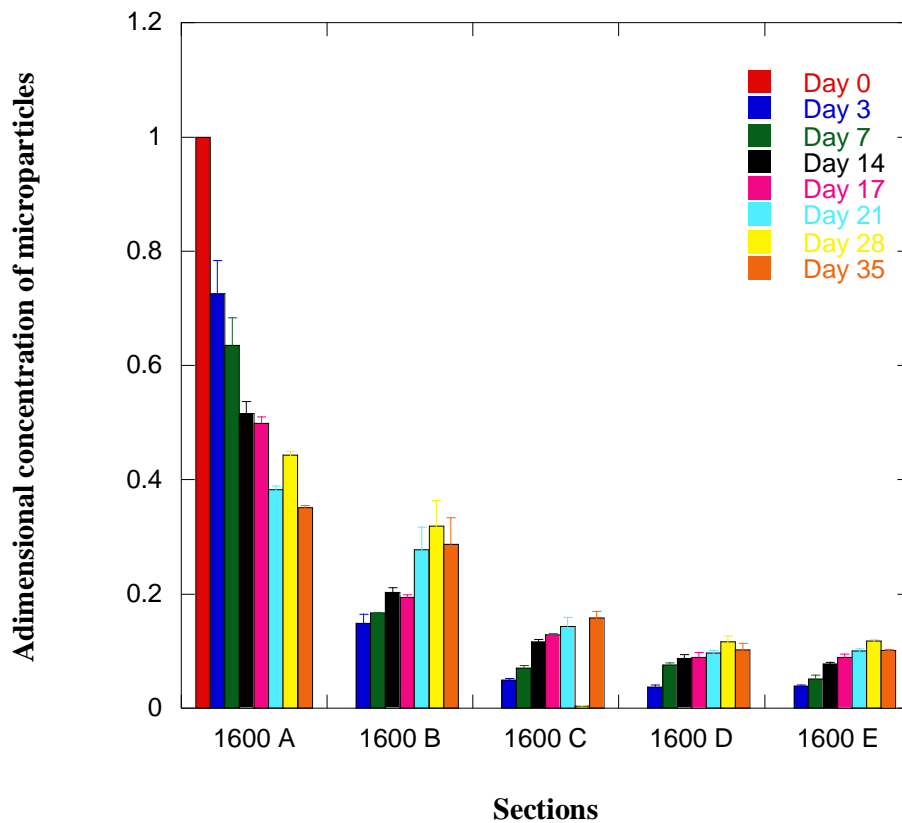
324
325

Figure 7: Diffusion test of HA1600 MPs.

326 The obtained results have shown that the MPs made up of bare PLGA diffuse in SVB faster than
 327 those decorated superficially with HA and also that, by increasing the molecular weight of the latter
 328 on MP surface corona, MP diffusion through the various sections in which the syringe has been
 329 previously divided is further hampered. More in detail, after 35 days, bare PLGA MPs diffuse from
 330 section A of the syringe (in which the MPs were initially loaded) to section E and are uniformly
 331 distributed through the syringe sections. Differently, after 35 days in section E there are ~16% and
 332 ~10% of HA180 and HA1600 MPs initially loaded in section A, respectively. The difference in
 333 diffusivity between MP formulations can be confidently attributed to the presence of HA on the
 334 surface of MPs. In fact, it is possible to hypothesize that HA exposes the terminal of the polymeric
 335 chain outside the MP, thus favoring the interactions with the simulated vitreous body, containing
 336 the same polysaccharide, and thus slowing down the transport of the MPs. Furthermore, the
 337 different conformations assumed by HA of different molecular weight affects both the number and

338 the entities of the physical entanglements made with HA macromolecules present in the simulated
339 vitreous, thus further modulating the diffusion kinetics of MPs. Therefore, HA1600 MPs, exposing
340 longer HA chains on their surface, show a more hindered transport in SVB. This is expected to limit
341 their aggregation once injected intravitreally, thus improving their ability to control and prolong
342 drug release.

343

344

345 **4. Conclusions**

346 The aim of this work was the production of biodegradable PLGA-based MPs, with tailored surface
347 properties so as to be motionless within the vitreal space. More in detail, MP surface has been
348 decorated with HA with different molecular weight (180 and 1600 KDa), which is also a main
349 constituent of the vitreous body. The chemical composition affinity between MP surface and the
350 vitreous body proved to be efficacious in slowing down MP diffusion into SVB and the different
351 length of HA chains on MP surface, proved to be an effective tool to further modulate the transport
352 of MPs in SVB. Moreover, HA MPs presented a prolonged degradation time compared to bare
353 PLGA MPs that, in turn, contribute to sustain the release of the loaded drug molecule(s), thereby
354 reducing the frequency of intravitreal injections and the related risk of adverse effects. The different
355 molecular weight of the biopolymer on MP corona does not greatly affect the degradation time of
356 the MPs while can modulate the amount of protein released by the devices. Taken altogether, these
357 outcomes shows the attractiveness of these systems for the intraocular delivery of therapeutic
358 proteins.

359

5. References

- 361 Blasi P, D'Souza SS, Selmin F, DeLuca PP. Plasticizing effect of water on poly(lactide-co-
362 glycolide). *J Control Release*. 2005;108(1):1-9.
- 363 Borzacchiello, A., Mayol, L., Schiavinato, A., Ambrosio, L. (2010). Effect of hyaluronic acid
364 amide derivative on equine synovial fluid viscoelasticity. *Journal of Biomedical Materials Research*
365 *Part A*, 92, 1162-1170.
- 366 Danhier, F., Ansorena, E., Silva, J.M., Coco, R., Le Breton, A., Préat, V. (2012). PLGA-based
367 nanoparticles: an overview of biomedical applications. *J Control Release*, 161, 505-22.
- 368 Falavarjani, K.G. and Nguyen, Q.D. (2013). Adverse events and complications associated with
369 intravitreal injection of anti-VEGF agents: a review of literature. *Eye*, 27, 787-794.
- 370 Gaudana, R., Ananthula, H. K., Parenky, A., Mitra, A.K. (2010). Ocular Drug Delivery. *American*
371 *Association of Pharmaceutical Scientist Journal*, 12, 348-360.
- 372 Giarra, S., Serri, C., Russo, L., Zeppetelli, S., De Rosa, G., Borzacchiello, A., Biondi, M.,
373 Ambrosio, L., Mayol, L. (2016). Spontaneous arrangement of a tumor targeting hyaluronic acid
374 shell on irinotecan loaded PLGA nanoparticles. *Carbohydrate Polymers*;140:400-7.
- 375 Herrero-Vanrell R, L., Ramirez, A., Fernandez-Carballido, Refojo, M.F. (2000). Biodegradable
376 PLGA microspheres loaded with ganciclovir for intraocular administration. Encapsulation
377 technique, in vitro release profiles, and sterilization process. *Pharmaceutical Research*, 17, 1323-
378 1328.
- 379 Herrero-Vanrell, R. and Refojo, M.F. (2001). Biodegradable microspheres for vitreoretinal drug
380 delivery. *Advanced Drug Delivery Review*, 52, 5-16.
- 381 Herrero-Vanrell, R., Bravo-Osuna, I., Andres-Guerrero, V., Vicario-de-la-Torre, M., Molina-
382 Martinez, I.T. (2014). The potential of using biodegradable microspheres in retinal diseases and
383 other intraocular pathologies, *Progress in Retinal Eye Research*, 42, 27-43.

384 Joshi A, Himmelstein KJ. Dynamics of controlled release from bioerodible matrices. *Journal of*
385 *Controlled Release*. 1991;15(2):95–104.

386 Kummer, M.P., Abbott, J.J., Dinser, S., Nelson, B.J. (2007). Artificial vitreous humor for in vitro
387 experiments. *Conf Proc IEEE Eng Med Biol Soc*. 2007, 6407-10.

388 Mayol et al., 2014 *Journal of Materials Science: Materials in Medicine* February 2014, Volume 25,
389 Issue 2, pp 383–390 Design of electrosprayed non-spherical poly (l-lactide-co-glicolide)
390 microdevices for sustained drug delivery.

391 Mayol L, Serri C, Menale C, Crispi S, Piccolo MT, Mita L, Giarra S, Forte M, Saija A, Biondi M,
392 Mita DG. Curcumin loaded PLGA-poloxamer blend nanoparticles induce cell cycle arrest in
393 mesothelioma cells. *Eur J Pharm Biopharm*. 2015;93:37-45.

394 Mayol L, De Stefano D, De Falco F, Carnuccio R, Maiuri MC, De Rosa G. Effect of hyaluronic
395 acid on the thermogelation and biocompatibility of its blends with methyl cellulose. *Carbohydr*
396 *Polym*. 2014;112:480-5.

397 Noble JE, Bailey MJ. Quantitation of protein. *Methods Enzymol*. 2009;463:73-95.

398 Schugens C, Laurelle N, Nihant N, Grandfils C, JérômeR, Teyssié P. Effect of the emulsion
399 stability on the morphology and porosity of semicrystalline poly l-lactide microparticles prepared
400 by w/o/w double emulsion-evaporation. *J. Control. Release*, 32 (1994), 161-76

401 Serri C, Argirò M, Piras L, Mita DG, Saija A, Mita L, Forte M, Giarra S, Biondi M, Crispi S,
402 Mayol L. Nano-precipitated curcumin loaded particles: effect of carrier size and drug complexation
403 with (2-hydroxypropyl)- β -cyclodextrin on their biological performances. *Int J Pharm*. 2017;520:21-
404 28.

405 Serri C, Quagliariello V, Iaffaioli RV, Fusco S, Botti G, Mayol L, Biondi M. Combination therapy
406 for the treatment of pancreatic cancer through hyaluronic acid-decorated nanoparticles loaded with
407 quercetin and gemcitabine: A preliminary in vitro study. *J Cell Physiol*. 2019;234(4):4959-4969.

408 Soman N, Banerjee R. Artificial vitreous replacements. *Biomed Mater Eng*. 2003;13(1):59-74.

409 Tamada JA, Langer R. Erosion kinetics of hydrolytically degradable polymers, Proc. Natl. Acad.
410 Sci. USA 90 (1992) 552-556.

411 Ungaro F, Biondi M, d'Angelo I, Indolfi L, Quaglia F, Netti PA, La Rotonda MI. Microsphere-
412 integrated collagen scaffolds for tissue engineering: effect of microsphere formulation and scaffold
413 properties on protein release kinetics. J Control Release. 2006 Jun 28;113(2):128-36.

414 Wang C, Hou H, Nan K, Sailor MJ, Freeman WR, Cheng L. Intravitreal controlled release of
415 dexamethasone from engineered microparticles of porous silicon dioxide. Exp Eye Res.
416 2014;129:74-82.

417 Xu Q, Boylan NJ, Suk JS, Wang YY, Nance EA, Yang JC, McDonnell PJ, Cone RA, Duh EJ,
418 Hanes J. Nanoparticle diffusion in, and microrheology of, the bovine vitreous ex vivo. J Control
419 Release. 2013;167:76-84.

420 Yasukawa T, Y. Tabata, H. Kimura, and Y. Ogura, 2011, Recent advances in intraocular drug
421 delivery systems, Recent Patents on Drug Delivery & Formulation, 5, 1-10.

422 Zhang L, Si T, Fischer AJ, Letson A, Yuan S, Roberts CJ, Xu RX. Coaxial Electrospray of
423 Ranibizumab-Loaded Microparticles for Sustained Release of Anti-VEGF Therapies. PLoS One.
424 2015;10(8):e0135608.

425

426